Inside Cover

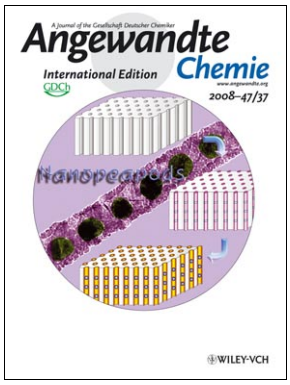

Lifeng Liu,* Woo Lee,* Roland Scholz, Eckhard Pippel, and Ulrich Gösele

Pt@CoAl2O4 inorganic nanopeapods consisting of well-defined platinum nanoparticle chains embedded in $CoAl_2O_4$ nanoshells are synthesized "à la carte" by an approach combining template-based electrodeposition with a high-temperature solid-state reaction route, as described by L. Liu et al. in their Communication on page 7004 ff. The size, separation, and arrangement of platinum nanoparticles can be tuned easily. The nanopeapods are promising building blocks for nanoscale photonic devices.

Nanoparticle Chains

DOI: 10.1002/anie.200801931

Tailor-Made Inorganic Nanopeapods: Structural Design of Linear Noble Metal Nanoparticle Chains

Lifeng Liu, Woo Lee,* Roland Scholz, Eckhard Pippel, and Ulrich Gösele*

Linear noble-metal nanoparticle (NP) chains have been demonstrated both theoretically and experimentally to be promising candidates for applications in one-dimensional nano-optical devices (e.g. plasmonic waveguides, plasmonic printing).[1–4] The ability of metal NP chains to transport electromagnetic energy below the diffraction limit has major advantages for scaling down the size of optical devices and components to the nanometer scale. Precise control of particle size, shape and separation in metal NP chains is an important issue for constructing nano-optical devices. Conventional electron-beam lithographic techniques and scanning-probe manipulation have enabled excellent control over the size and position of metal NPs but are time-consuming and costly.[2,5] Self-assembly routes enable metal NPs to be incorporated into preformed grooves but can control neither the separation between NPs nor their densities.[6] Other approaches to the fabrication of metal NP chains, including wet-chemistry etching[7] and exploitation of the Rayleigh instability of metal nanowires (NWs),[8] suffer from low throughput and limited controllability. Herein, we show a facile and controllable route to the fabrication of linear noble-metal NP chains, in which the size and the separation of optically interesting NPs can be controlled easily. As an example, Pt@$CoAl_2O_4$ inorganic peapod nanostructures, which consist of well-defined Pt NPs encapsulated in continuous $CoAl_2O_4$ nanoshells, were realized by electrodeposition of cobalt/platinum multilayered (ML) NWs into nanoporous anodic aluminum oxide (AAO) membranes and subsequent solid-state reaction at high temperature.

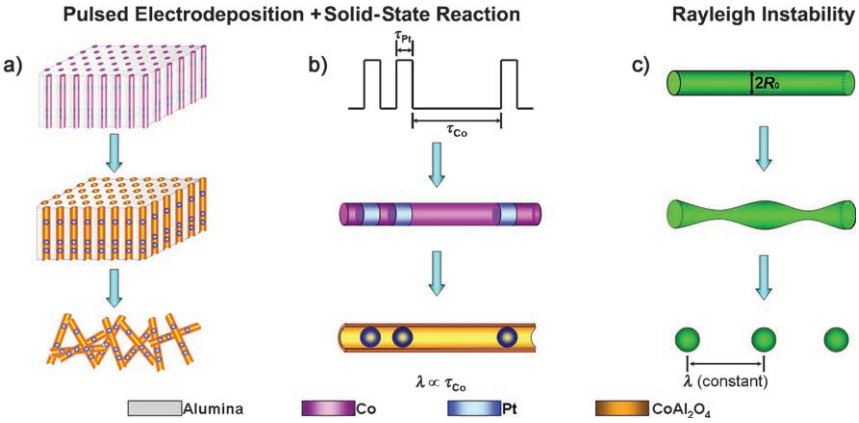

Figure 1. Fabrication of peapod nanostructures. a, b) Fabrication of Pt@$CoAl_2O_4$ inorganic nanopeapods (Pt nanoparticle chains encapsulated in $CoAl_2O_4$ nanoshells) by template-based pulsed electrodeposition and high-temperature solid-state reaction. The separation between Pt nanoparticles ($D_{c\text{-}c}$) is proportional to the pulse duration for Co electrodeposition, τ_{Co}, and can be changed at will. c) Metal nanoparticle chains fabricated on the basis of the Rayleigh instability of metal nanowires.[8b]

Fabrication of Pt@$CoAl_2O_4$ inorganic nanopeapods is schematically illustrated in Figure 1a. First, Co/Pt ML NWs were electrodeposited into the nanoporous AAO template by pulsed potential electrodeposition. As-prepared Co/Pt ML NWs with alternately distributed Co and Pt segments served as the precursors and the backbones for subsequent generation of Pt@$CoAl_2O_4$ inorganic nanopeapods (see Figure S1 in the Supporting Information). The size (diameter, D_{Pt}) and separation (center-to-center distance, $D_{c\text{-}c}$) of Pt "peas" in peapod nanostructures were also defined in this step by the lengths of Pt (L_{Pt}) and Co segments (L_{Co}), respectively. After electrodeposition, the Co/Pt ML NWs/AAO composite membrane was annealed at 700 °C in an ambient atmosphere for 1–5 h. During heat treatment, Co segments reacted with alumina to form continuous $CoAl_2O_4$ nanoshells, that is, the "pods", while most Pt segments agglomerated into a spherical shape to minimize their surface energy, forming the peas. Thus, the peapod nanostructures were obtained. As-prepared Pt@$CoAl_2O_4$ inorganic nanopeapods can either be kept in the porous AAO template or be easily released from the template by selectively removing the surrounding alumina (see Figure S2a in the Supporting Information).

Recently, exploitation of the Rayleigh instability of metal NWs has been considered as an effective "bottom-up" approach to create linear metal NP chains.[8,9] However, this method only allows very limited control of the separation between metal NPs. Its controlling capability is strictly confined by the maximum perturbation wavelength λ_{max}, which is directly proportional to the radius R_0 of the metal NWs used, as shown in Figure 1c. The proportionality

[*] Dr. L. Liu, Dr. W. Lee, Dr. R. Scholz, Dr. E. Pippel, Prof. U. Gösele
Max Planck Institute of Microstructure Physics
Weinberg 2, 06120 Halle (Germany)
E-mail: liulif@mpi-halle.de
Dr. W. Lee
Korea Research Institute of Standards and Science (KRISS)
Yuseong, Daejon 305-340 (Korea)
E-mail: woolee@kriss.re.kr

Supporting information for this article is available on the WWW under http://dx.doi.org/10.1002/anie.200801931.

InterScience
© 2008 Wiley-VCH Verlag GmbH & Co. KGaA, Weinheim

constants are fixed to values equal to $\sqrt{2}\times 2\pi$, $1.43\times 2\pi$, and $2.06\times 2\pi$ for surface diffusion, internal volume diffusion, and external volume diffusion,[8c] respectively. The invariable separation between NPs reduces the degree of freedom in most practical applications, especially in plasmonic applications. In contrast, in our approach the aspect ratio and the separation of metal NPs can easily be tailored without major limitations by virtue of the generic controllability of the diameter of nanopores of the alumina membrane used and of the length of metal segments by adjusting the pulse durations in electrodeposition. For an alumina template with a given pore diameter, the size (D_{Pt}) and separation ($D_{c\text{-}c}$) of metal peas are roughly proportional to the pulse durations for Pt (τ_{Pt}) and Co (τ_{Co}) electrodeposition, respectively, and can be changed at will (Figure 1b). Moreover, tailor-made peapod nanostructures with designed optical defects in periodically arranged chains of NPs can be easily realized by deliberately designing the pulse sequences, which will potentially enable systematic studies on plasmonic interactions between optically interesting metal NPs (e.g., Ag, Au, and Pt) in various geometric configurations.

Figure 2a displays a representative TEM micrograph of a single Pt@$CoAl_2O_4$ inorganic nanopeapod prepared from

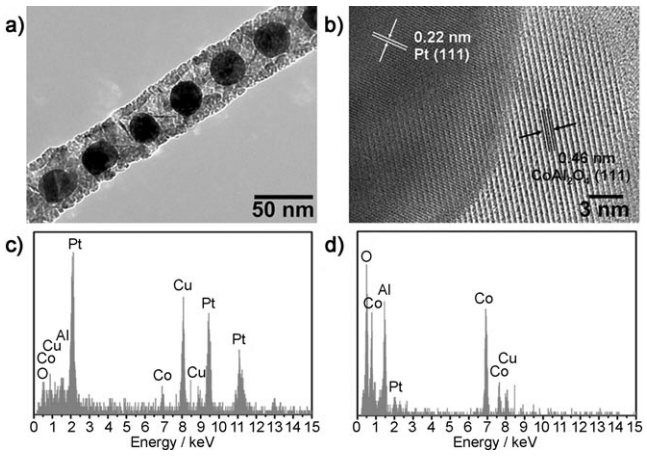

Figure 2. Pt@$CoAl_2O_4$ inorganic nanopeapods. a) TEM image of a single inorganic nanopeapod. b) HRTEM image of a Pt@$CoAl_2O_4$ inorganic nanopeapod. c,d) EDX spectra collected from the pea and the pod part of the structure, respectively.

$H_2C_2O_4$-anodized AAO, which exhibits clearly alternating dark and bright image contrasts. It is evident that the Pt peas are relatively regular spheres, and the oxide pods consist of many nanocrystallites. In this specific sample, the size (D_{Pt}) and the separation ($D_{c\text{-}c}$) of Pt peas average 28 and 45 nm, respectively. Previously solid Co segments have been converted into hollow oxide nanoshells, manifesting a solid-state reaction between the metallic Co segments and the pore walls of the alumina template during the annealing of the sample at 700 °C. Electron diffraction analysis reveals that as-prepared peapod nanostructures contain two phases (see Figure S2b in the Supporting Information). The one phase can be determined to be metallic platinum; the other is $CoAl_2O_4$. High-resolution transmission electron microscopy (HRTEM) investigations reveal clearly that the present inorganic peapod nanostructures consist of highly crystalline metallic Pt peas and $CoAl_2O_4$ pods (Figure 2b). Energy dispersive X-ray (EDX) elemental analyses also confirmed that the pea part is composed of Pt as a major component and of Co, Al, and O as minor components stemming from the pod shell surrounding the peas (Figure 2c); the pod part of the structure contains Co, Al, and O as major components (Figure 2d). The small amount of Pt detected from the pod could be attributed to inelastic electron scattering by the pea. The atomic ratio of Co to Al was 1:2.3, close to that of stoichiometric $CoAl_2O_4$. The tubular nature of $CoAl_2O_4$ was further confirmed by a radial elemental linescan along the pod and elemental mapping analyses (see Figure S3 in the Supporting Information).

Figure 3 demonstrates that the size (D_{Pt}) and the separation ($D_{c\text{-}c}$) of Pt peas can be readily controlled using AAO membranes with different pore diameters and by adjusting

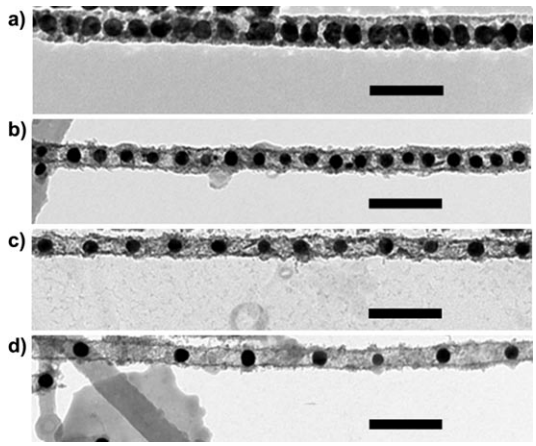

Figure 3. TEM micrographs of Pt@$CoAl_2O_4$ inorganic nanopeapods with different pea sizes (D_{Pt}) and separations ($D_{c\text{-}c}$) manifest facile control of these physical dimensions. The Co/Pt multilayered nanowires were prepared by different pulse durations: a) $\tau_{Co}=6$ s, $\tau_{Pt}=25$ s (**S1**); b) $\tau_{Co}=8$ s, $\tau_{Pt}=18$ s (**S2**); c) $\tau_{Co}=10$ s, $\tau_{Pt}=18$ s (**S3**); d) $\tau_{Co}=12$ s, $\tau_{Pt}=15$ s (**S4**). **S1** was prepared in a $H_2C_2O_4$-anodized AAO, while **S2**, **S3**, and **S4** were prepared in H_2SO_4-anodized AAO. The scale bars are 100 nm.

the pulse durations for Pt and Co electrodepositions, τ_{Pt} and τ_{Co}. A Pt@$CoAl_2O_4$ inorganic nanopeapod prepared using a $H_2C_2O_4$-anodized AAO membrane (Sample **S1**) is shown in Figure 3a. The Co/Pt ML NW precursor was electrodeposited with pulse durations $\tau_{Pt}=25$ s and $\tau_{Co}=6$ s. In this specific inorganic nanopeapod, the diameter of Pt peas is 25.6 ± 1.6 nm, and the separation is 29.0 ± 2.9 nm. The inorganic nanopeapods presented in Figure 3b–d were prepared using H_2SO_4-anodized AAO membranes, but with different deposition pulse durations for Pt and Co: $\tau_{Pt}=18$ s and $\tau_{Co}=8$ s for Figure 3b (Sample **S2**), $\tau_{Pt}=18$ s and $\tau_{Co}=10$ s for Figure 3c (Sample **S3**), and $\tau_{Pt}=15$ s and $\tau_{Co}=12$ s for Figure 3d (Sample **S4**). It is clear that the sizes (D_{Pt}) of the Pt peas are typically smaller than those prepared from $H_2C_2O_4$-anodized AAO membranes. Moreover, the separations ($D_{c\text{-}c}$) of Pt peas are roughly proportional to the Co pulse durations,

 © 2008 Wiley-VCH Verlag GmbH & Co. KGaA, Weinheim

τ_{Co}. Statistical analyses demonstrate that pea size (D_{Pt}) and separation ($D_{c\text{-}c}$) variations in all these samples are less than 10 and 15%, respectively, (see Figures S4 and S5 and Table S1 in the Supporting Information), indicating good controllability.

In addition to Pt@$CoAl_2O_4$ inorganic nanopeapods with regular pea separations, periodically modulated peapod nanostructures can also be realized by applying different

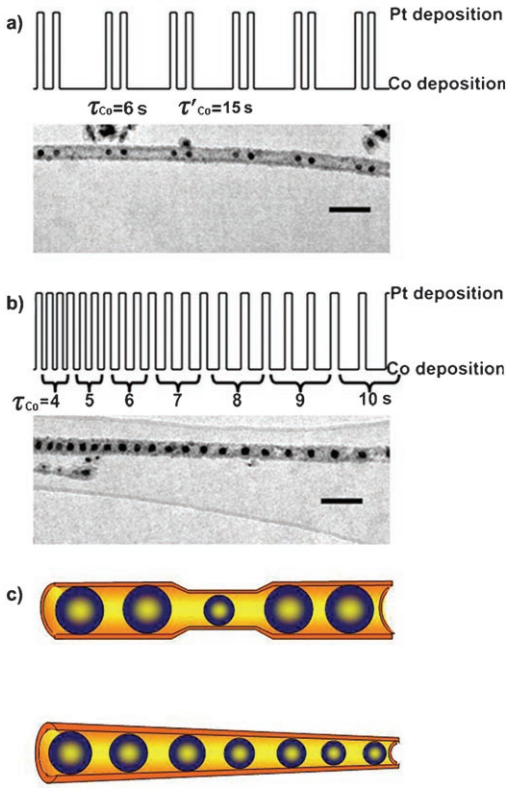

Figure 4. Structural engineering of Pt@$CoAl_2O_4$ inorganic nanopeapods. a) Inorganic nanopeapods with periodically distributed Pt nanoparticle pairs. b) Inorganic nanopeapods with gradually increasing separations between Pt peas (from left to right). The scale bars are 200 nm. c) Conceptual illustration of diameter-modulated inorganic nanopeapods prepared with diameter-modulated AAO membranes.

pulse waveforms during the electrodeposition. Figure 4a shows a TEM image of one inorganic nanopeapod prepared by successively applying double pulses: $\tau_{Pt} = 18$ s, $\tau_{Co} = 6$ s and $\tau'_{Pt} = 18$ s, $\tau'_{Co} = 15$ s. Two metal Pt NPs form a set of metal peas with a well-defined distance between the two NPs. These sets are embedded in a $CoAl_2O_4$ nanoshell with a regular separation. Figure 4b is another example showing a peapod nanostructure with gradually increasing separations between the peas (from left to right). This nanopeapod arrangement was prepared by continuously changing the pulse durations τ_{Co}. Moreover, it can be imagined that if AAO membranes with periodically modulated diameters[10] or with a continuously changing diameter[11] are employed, diameter-modulated inorganic nanopeapods could also be realized, as illustrated conceptually in Figure 4c. These diameter-modulated inorganic nanopeapods may find potential application in plasmonic focusing.[12]

To gain insight into the formation mechanism of Pt@$CoAl_2O_4$ inorganic nanopeapods, we performed a series of control experiments by annealing the as-prepared Co/Pt ML NWs/AAO composites at different conditions. The morphol-

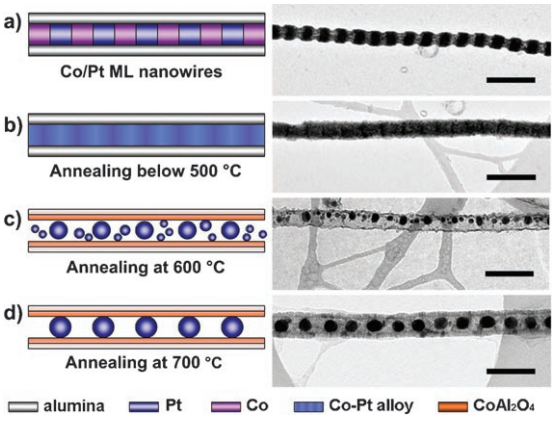

Figure 5. TEM micrographs of Co/Pt ML nanowires annealed at different temperatures in air for 4 h. a) As-prepared. b) Below 500 °C. At this stage, intermetallic alloying takes place, and the interfaces between different metal segments become blurred. c) 600 °C. $CoAl_2O_4$ nanoshells emerge. d) 700 °C. Pt@$CoAl_2O_4$ inorganic nanopeapods with structurally well-defined Pt peas are formed. The scale bars are 100 nm.

ogy of the resulting nanostructures was found to be sensitive to the atmosphere and the annealing temperature (Figure 5). When the sample was annealed in air below 500 °C, intermetallic alloying between Co and Pt occurred preferentially to form continuous CoPt alloy NWs (Figure 5b). When the sample was annealed at 600 °C, $CoAl_2O_4$ nanoshells started to emerge as the result of a solid-state reaction between metallic Co and the alumina pore walls. The resulting nanostructures were characterized as continuous $CoAl_2O_4$ pods containing randomly distributed Pt peas (Figure 5c). The size of Pt peas appeared to be non-uniform. The formation of hollow nanotubes of ternary compounds starting from a solid nanowire (ZnO) covered by an amorphous shell of Al_2O_3 has been reported recently[13] and was attributed to the nanoscale Kirkendall effect.[14] An analogous mechanism appears to operate in the present case of Co surrounded by Al_2O_3. We assume that two interfacial reactions take place competitively at the early stage of annealing: 1) the reaction between Co and Al_2O_3 at the interface of Co segments and the pore walls of alumina, 2) the intermetallic alloying at the interface of Co and Pt segments. As the reaction proceeds, however, dealloying of the CoPt alloy takes place to form the thermodynamically more stable $CoAl_2O_4$ phase (i.e., at 600 °C), resulting in randomly distributed Pt NPs within tubular $CoAl_2O_4$ nanoshells. In other words, the early-stage reactions are mostly driven by kinetics, while the later stage is determined by thermodynamics. We believe that the net diffusion of Co metals into the pore walls of alumina results in the hollow $CoAl_2O_4$ nanoshells (pods). When the sample was directly heated to 700 °C, structurally well-defined Pt@

 © 2008 Wiley-VCH Verlag GmbH & Co. KGaA, Weinheim

$CoAl_2O_4$ peapod nanostructures without any randomly distributed Pt NPs formed exclusively (Figure 5d). This result indicates that, under these annealing conditions (i.e., in air at 700 °C), the formation of $CoAl_2O_4$ nanoshells by the diffusion of Co metal into the Al_2O_3 lattice is kinetically and thermodynamically more favorable than the intermetallic alloying between Co and Pt.

To check any possible contribution of oxygen in air to the formation of Pt@$CoAl_2O_4$ nanopeapods, as-prepared Co/Pt ML NWs/AAO composite was annealed at 700 °C under argon atmosphere. We obtained Pt@$CoAl_2O_4$ peapod nanostructures even in this oxygen-deficient atmosphere. However, the size and the distribution of Pt peas were nonuniform, similar to the case of annealing in air at 600 °C (Figure S6). This control experiment discloses that the annealing atmosphere has less impact on the formation of inorganic peapod nanostructures than the AAO membrane, but the oxygen atmosphere can effectively hinder the alloying process and accelerate the formation of $CoAl_2O_4$.

As discussed above, the AAO template serves as a reactant and plays an important role in the formation of $CoAl_2O_4$ nanoshells (pods) during the high-temperature annealing of Co/Pt ML NWs/AAO composite in air. It has been well-documented that the pore walls of anodic alumina consist of two main layers (a relatively pure inner oxide layer and an anion-contaminated outer oxide layer).[10,15] The outer layer, the surface of which comes in contact with the Co/Pt ML NWs in the present study, is mainly characterized as amorphous aluminum oxide, containing anions from the electrolyte used in anodization (such as OH^- from water, SO_4^{2-} from H_2SO_4, $C_2O_4^{2-}$ from $H_2C_2O_4$, or PO_4^{3-} from H_3PO_4).[10,16] It is believed that Co at the surface of anodic alumina is partially oxidized to CoO by reacting with the oxygen released from the AAO template,[17] with subsequent solid-state diffusion of CoO into Al_2O_3 lattice to form $CoAl_2O_4$,[18] that is, the reactions shown in Equation (1) could occur.

$$\begin{aligned} Co + O &\rightarrow CoO \\ CoO + Al_2O_3 &\rightarrow CoAl_2O_4 \end{aligned} \quad (1)$$

In fact, a previous study showed that calcination of CoO/Al_2O_3 composite catalysts above 600 °C appears to cause gradual diffusion of CoO into alumina, thus resulting in the formation of $CoAl_2O_4$.[19] Moreover, water has been found to facilitate migration of Co into alumina to form $CoAl_2O_4$ by increasing the interaction between Co and Al_2O_3.[18c,20]

In summary, Pt@$CoAl_2O_4$ inorganic nanopeapods with designed separations between the Pt nanoparticles were synthesized. Combination of pulsed electrodeposition of multilayered metal nanowires into anodic aluminum oxide membranes and a subsequent solid-state reaction between metals and alumina provides a facile and controllable way for the realization of noble metal@oxide inorganic peapod nanostructures. The present synthetic approach could also easily be extended to the fabrication of other metal@oxide inorganic nanopeapods.

Experimental Section

Membrane preparation: The AAO membranes were prepared by a two-step process reported previously.[21] Briefly, high-purity aluminum sheets (99.999%) were first electropolished in a mixture of $HClO_4$ and C_2H_5OH (1:3 v/v) for 4 min. The polished Al sheets were anodized in 0.3 M $H_2C_2O_4$ at 40 V or 0.3 M H_2SO_4 at 25 V at 1 °C. The first anodization was usually carried out for 20 h. Subsequently, the anodized Al sheets were put into an acid mixture (6 wt% H_3PO_4 and 1.8 wt% CrO_3) to completely remove the porous layer. Then, the second anodization was conducted for 16 h at the same conditions as the first anodization. Free-standing alumina membranes were obtained by a stepwise voltage reduction technique. The nominal pore diameters of as-prepared membranes were 45 ± 5 nm for $H_2C_2O_4$ anodization and 30 nm for H_2SO_4 anodization.

Electrodeposition of Co/Pt multilayered nanowires: Before electrodeposition, a layer of gold was sputtered on one side of the AAO membrane to make the surface electrically conductive. The electrodeposition was carried out in a standard three-electrode electrochemical cell. Gold-coated AAO and a platinum mesh were used as working electrode and counter electrode, respectively, and a saturated calomel electrode (SCE) served as a reference. The electrolyte consisted of 0.3 M $CoCl_2 \cdot 6H_2O$ (Sigma), 0.01 M K_2PtCl_6 (Sigma), and 0.485 M H_3BO_3 (Aldrich), with >18 MΩ deionized water. The deposition potential was controlled to periodically switch between −0.3 V (vs. SCE) for Pt deposition and −1.0 V (vs. SCE) for Co deposition by a Princeton Applied Research potentiostat (PAR 263 A). The number of deposition cycles was typically in the range of 200–300.

Fabrication of Pt@$CoAl_2O_4$ nanopeapods: As-prepared Co/Pt ML NWs/AAO membrane composite was heated on a hot plate in air. The temperature of the hot plate was ramped to 700 °C within 10 min and then was maintained for 1–5 h. Subsequently, the sample was cooled to room temperature. In the control experiments, Co/Pt ML NWs/AAO composites were annealed in air at different temperatures and annealed in argon atmosphere (100 mL min^{-1}, high-purity Ar, 99.99%). In all experiments, the temperature was rapidly increased to a set value within 10 min.

Characterization of Pt@$CoAl_2O_4$ nanopeapods: The normal TEM characterization was performed with a JEOL JEM-1010 transmission electron microscope, and HRTEM and EDX examinations were carried out by using JEOL JEM-4010, Philips CM20FEG, and FEI TITAN 80–300 microscopes. For TEM investigations, the samples were immersed in 2 M NaOH solution at 45 °C for several hours to completely remove alumina. The product was then washed with a large amount of deionized water and finally was dispersed in absolute ethanol. Subsequently, a drop of the suspension was placed on a carbon-coated copper grid for examination.

Received: April 24, 2008
Revised: June 12, 2008
Published online: July 28, 2008

Keywords: electrochemistry · nanostructures · platinum · solid-state reactions · template synthesis

[1] M. Quinten, A. Leitner, J. R. Krenn, F. R. Aussenegg, *Opt. Lett.* **1998**, *23*, 1331–1333.
[2] a) S. A. Maier, M. L. Brongersma, P. G. Kik, S. Meltzer, A. A. G. Requicha, H. A. Atwater, *Adv. Mater.* **2001**, *13*, 1501–1505; b) S. A. Maier, M. L. Brongersma, P. G. Kik, H. A. Atwater, *Phys. Rev. B* **2002**, *65*, 193408; c) S. A. Maier, P. G. Kik, H. A. Atwater, S. Meltzer, E. Harel, B. E. Koel, A. A. G. Requicha, *Nat. Mater.* **2003**, *2*, 229–232.
[3] M. Derouard, J. Hazart, G. Lerondel, R. Bachelot, P. M. Adam, P. Royer, *Opt. Express* **2007**, *15*, 4238–4246.

 © 2008 Wiley-VCH Verlag GmbH & Co. KGaA, Weinheim

[4] L. Qin, M. J. Banholzer, J. E. Millstone, C. A. Mirkin, *Nano Lett.* **2007**, *7*, 3849 – 3853.
[5] Q. H. Wei, K. H. Su, S. Durant, X. Zhang, *Nano Lett.* **2004**, *4*, 1067 – 1071.
[6] Y. Lu, Y. D. Yin, Z. Y. Li, Y. Xia, *Nano Lett.* **2002**, *2*, 785 – 788.
[7] a) J. A. Sioss, C. D. Keating, *Nano Lett.* **2005**, *5*, 1779 – 1783; b) L. D. Qin, S. Park, L. Huang, C. A. Mirkin, *Science* **2005**, *309*, 113 – 115; c) S. H. Liu, J. B. H. Tok, Z. N. Bao, *Nano Lett.* **2005**, *5*, 1071 – 1076; d) S. E. Hunyadi, C. J. Murphy, *J. Phys. Chem. B* **2006**, *110*, 7226 – 7231.
[8] a) M. E. Toimil-Molares, A. G. Balogh, T. W. Cornelius, R. Neumann, C. Trautmann, *Appl. Phys. Lett.* **2004**, *85*, 5337 – 5339; b) S. Karim, M. E. Toimil-Morlares, A. G. Balogh, W. Ensinger, T. W. Cornelius, E. U. Khan, R. Neumann, *Nanotechnology* **2006**, *17*, 5954 – 5959; c) S. Karim, M. E. Toimil-Molares, W. Ensinger, A. G. Balogh, T. W. Cornelius, E. U. Khan, R. Neumann, *J. Phys. D* **2007**, *40*, 3767 – 3770.
[9] Y. Qin, S. M. Lee, A. L. Pan, M. Knez, U. Gösele, *Nano Lett.* **2008**, *8*, 114 – 118.
[10] a) W. Lee, R. Ji, U. Gösele, K. Nielsch, *Nat. Mater.* **2006**, *5*, 741 – 747; b) W. Lee, K. Schwirn, M. Steinhart, E. Pippel, R. Scholz, U. Gösele, *Nat. Nanotechnol.* **2008**, *3*, 234 – 239.
[11] B. He, S. J. Son, S. B. Lee, *Anal. Chem.* **2007**, *79*, 5257 – 5263.
[12] S. Bidault, F. J. G. de Abajo, A. Polman, *J. Am. Chem. Soc.* **2008**, *130*, 2750 – 2751.
[13] H. Jin Fan, M. Knez, R. Scholz, K. Nielsch, E. Pipple, D. Hesse, M. Zacharias, U. Gösele, *Nat. Mater.* **2006**, *5*, 627 – 631.
[14] Y. D. Yin, R. M. Rioux, C. K. Erdonmez, S. Hughes, G. A. Somorjai, A. P. Alivisatos, *Science* **2004**, *304*, 711 – 714.
[15] G. E. Thompson, G. C. Wood, *Nature* **1981**, *290*, 230 – 232.
[16] a) S. Ono, N. Masuko, *Corros. Sci.* **1992**, *33*, 503 – 507; b) J. W. Diggle, T. C. Downie, C. W. Goulding, *Chem. Rev.* **1969**, *69*, 365 – 405.
[17] L. Li, Y. W. Yang, G. H. Li, L. D. Zhang, *Small* **2006**, *2*, 548 – 553.
[18] a) S. Chokkaram, R. Srinivasan, D. R. Milburn, B. H. Davis, *J. Mol. Catal. A* **1997**, *121*, 157 – 169; b) P. H. Bolt, F. Habraken, J. W. Geus, *J. Solid State Chem.* **1998**, *135*, 59 – 69; c) A. Sirijaruphan, A. Horvath, J. G. Goodwin, R. Oukaci, *Catal. Lett.* **2003**, *91*, 89 – 94.
[19] P. Arnoldy, J. A. Moulijn, *J. Catal.* **1985**, *93*, 38 – 54.
[20] a) Y. L. Zhang, D. G. Wei, S. Hammache, J. G. Goodwin, *J. Catal.* **1999**, *188*, 281 – 290; b) B. Jongsomjit, J. Panpranot, J. G. Goodwin, *J. Catal.* **2001**, *204*, 98 – 109.
[21] H. Masuda, M. Satoh, *Jpn. J. Appl. Phys.* **1996**, *35*, L126 – L129.

 © 2008 Wiley-VCH Verlag GmbH & Co. KGaA, Weinheim